# Gabor-Space Geodesic Active Contours

Chen Sagiv[1], Nir A. Sochen[1,2], and Yehoshua Y. Zeevi[1]

[1] Department of Electrical Engineering, Technion - Israel Institute of Technology
Technion City, Haifa 32000, Israel
chen@tiger.technion.ac.il, zeevi@ee.technion.ac.il
[2] Department of Applied Mathematics, University of Tel Aviv
Ramat-Aviv, Tel-Aviv 69978, Israel
sochen@math.tau.ac.il

**Abstract.** A novel scheme for texture segmentation is presented. Our algorithm is based on generalizing the intensity-based geodesic active contours model to the Gabor spatial-feature space of images. First, we apply the Gabor-Morlet transform to the image using self similar Gabor functions, and then implement the geodesic active snakes mechanism in this space. The spatial-feature space is represented, via the Beltrami framework, as a Riemannian manifold. The stopping term, in the geodesic snake mechanism, is generalized and is derived from the metric of the Gabor spatial-feature manifold. Experimental results obtained by applying the scheme to test images are presented.

**Keywords:** Texture segmentation, Gabor analysis, Geodesic active contours, Beltrami framework, Anisotropic diffusion, image manifolds.

## 1 Introduction

Image segmentation is an important issue in image analysis. Usually it is based on intensity features, e.g. gradients. However, real life images usually contain additional features such as textures and colors that determine image structure. In order to achieve texture segmentation (detecting the boundary between textural homogeneous regions), it is necessary to generalize the definition of segmentation to features other than intensity.

Since real world textures are difficult to model mathematically, no exact definition for texture exists. Therefore, ad-hoc approaches to the analysis of texture have been used, including local geometric primitives [8], local statistical features [3] and random field models [7,4]. A more general theory, based on the human visual system has emerged, in which texture features are extracted using Gabor filters [20].

The motivation for the use of Gabor filters in texture analysis is double folded. First, it is believed that simple cells in the visual cortex can be modeled by Gabor functions [16,5], and that the Gabor scheme provides a suitable representation for visual information in the combined frequency-position space [19]. Second, the Gabor representation has been shown to be optimal in the sense of minimizing the joint two-dimensional uncertainty in the combined spatial-frequency

G. Sommer and Y. Y. Zeevi (Eds.): AFPAC 2000, LNCS 1888, pp. 309–318, 2000.

space [6]. The analysis of Gabor filters was generalized to multi-window Gabor filters [23] and to Gabor-Morlet wavelets [19,23,17,12], and studied both analytically and experimentally on various classes of images [23]. A first attempt to use the Gabor feature space for segmentation was done by Lee et al [13] who use a variant of the Mumford-Shah functional adapted to some features in the Gabor space. Our method differs from theirs in using the entire information obtained by the Gabor analysis and in using a different segmentation technique.

In the last ten years, a great deal of attention was given to the "snakes", or active contours models which were proposed by Kaas et al [9] for intensity based image segmentation. In this framework an initial contour is deformed towards the boundary of an object to be detected. The evolution equation is derived from minimization of an energy functional, which obtains a minimum for a curve located at the boundary of the object.

The geodesic active contours model [2] offers a different perspective for solving the boundary detection problem; It is based on the observation that the energy minimization problem is equivalent to finding a geodesic curve in a Riemannian space whose metric is derived from image contents. The geodesic curve can be found via a geometric flow. Utilization of the Osher and Sethian level set numerical algorithm [21] allowed automatic handling of changes of topology.

It was shown recently that the Gaborian spatial-feature space can be described, via the Beltrami framework [22], as a 4D Riemannian manifold [11] embedded in $\mathbb{R}^6$. Based on this Riemannian structure we generalize the intensity based geodesic active contours method and apply it to the Gabor-feature space of images. Similar approaches, where the geodesic snakes scheme is applied to some feature space of the image, were studied by Lorigo et al [14] who used both intensity and its variance for MRI images' segmentation, and by Paragios et al [18] who generates the image's texture feature space by filtering the image using Gabor filters. Texture information is then expressed using statistical measurements. Texture segmentation is achieved by application of geodesic snakes to obtain the boundaries in the statistical feature space.

The aim of our study is to generalize the intensity-based geodesic active snakes method and apply it to the actual Gabor-feature space of images.

## 2 Geodesic Active Contours

In this section we review the geodesic active contours method for non-textured images [2]. The generalization of the technique for texture segmentation is described in section 4.

Let $\mathbf{C}(\mathbf{q}) : [0,1] \rightarrow \mathbb{R}^2$ be a parametrized curve, and let $I : [0,a] \times [0,b] \rightarrow \mathbb{R}^+$ be the given image. Let $E(r) : [0,\infty[ \rightarrow \mathbb{R}^+$ be an inverse edge detector, so that $E$ approaches zero when $r$ approaches infinity. Visually, $E$ should represent the edges in the image, so that we can judge the "quality" of the stopping term $E$ by the way it represents the edges and boundaries in an image. Thus, the stopping term $E$ has a fundamental role in the geodesic active snakes mechanism; if it does not well represents the edges, application of the snakes mechanism is likely to fail.

Minimizing the energy functional proposed in the classical snakes is generalized to finding a geodesic curve in a Riemannian space by minimizing:

$$L_R = \int E(|\nabla I(\mathbf{C}(q))|)\,|\mathbf{C}'(q)|dq. \tag{1}$$

We may see this term as a weighted length of a curve, where the Euclidean length element is weighted by $E(|\nabla I(C(q))|)$. The latter contains information regarding the boundaries in the image. The resultant evolution equation is the gradient descent flow:

$$\frac{\partial \mathbf{C}(t)}{\partial t} = E(|\nabla I|)k\mathbf{N} - (\nabla E \cdot \mathbf{N})\ \mathbf{N} \tag{2}$$

where $k$ denotes curvature.

If we now define a function $U$, so that $\mathbf{C} = ((x, y)|U(x, y) = 0)$, we may use the Osher-Sethian Level-Sets approach [21] and replace the evolution equation for the curve $\mathbf{C}$, with an evolution equation for the embedding function $U$:

$$\frac{\partial U(t)}{\partial t} = |\nabla U|\mathrm{Div}\left(E(|\nabla I|)\frac{\nabla U}{|\nabla U|}\right). \tag{3}$$

A popular choice for the stopping function $E(|\nabla I|)$ is given by:

$$E(I) = \frac{1}{1 + |\nabla I|^2}.$$

## 3 Feature Space and Gabor Transform

The Gabor scheme and Gabor filters have been studied by numerous researchers in the context of image representation, texture segmentation and image retrieval. A Gabor filter centered at the 2D frequency coordinates $(U, V)$ has the general form of:

$$h(x, y) = g(x', y')\exp(2\pi i(Ux + Vy)) \tag{4}$$

where

$$(x', y') = (x\cos(\phi) + y\sin(\phi), -x\sin(\phi) + y\cos(\phi)), \tag{5}$$

and

$$g(x, y) = \frac{1}{2\pi\sigma^2}\exp\left(-\frac{x^2}{2\lambda^2\sigma^2} - \frac{y^2}{2\sigma^2}\right) \tag{6}$$

where, $\lambda$ is the aspect ratio between x and y scales, $\sigma$ is the scale parameter, and the major axis of the Gaussian is oriented at angle $\phi$ relative to the x-axis and to the modulating sinewave gratings.

Accordingly, the Fourier transform of the Gabor function is:

$$H(u, v) = \exp\left(-2\pi^2\sigma^2((u' - U')^2\lambda^2 + (v' - V')^2)\right) \tag{7}$$

where, $(u', v')$ and $(U', V')$ are rotated frequency coordinates. Thus, $H(u, v)$ is a bandpass Gaussian with minor axis oriented at angle $\phi$ from the u-axis, and the radial center frequency $F$ is defined by : $F = U^2 + V^2$, with orientation $\theta = \arctan(V/U)$. Since maximal resolution in orientation is wanted, the filters whose sine gratings are cooriented with the major axis of the modulating Gaussian are usually considered ($\phi = \theta$ and $\lambda > 1$), and the Gabor filter is reduced to: $h(x, y) = g(x', y')exp(2\pi iFx')$.

It is possible to generate Gabor-Morlet wavelets from a single mother-Gabor-wavelet by transformations such as: translations, rotations and dilations. We can generate, in this way, a set of filters for a known number of scales, S, and orientations K. We obtain the following filters for a discrete subset of transformations: $h_{mn}(x, y) = a^{-m}g(x', y')$, where $(x', y')$ are the spatial coordinates rotated by $\frac{\pi n}{K}$ and $m = 0...S - 1$. Alternatively, one can obtain Gabor wavelets by logarithmicaly distorting the frequency axis [19] or by incorporating multiwindows [23]. In the latter case one obtains a more general scheme wherein subsets of the functions constitute either wavelet sets or Gaborian sets.

The feature space of an image is obtained by the inner product of this set of Gabor filters with the image:

$$W_{mn}(x, y) = R_{mn}(x, y) + iJ_{mn}(x, y) = I(x, y) * h_{mn}(x, y). \tag{8}$$

## 4 Application of Geodesic Snakes to the Gaborian Feature Space of Images

The proposed approach enables us to use the geodesic snakes mechanism in the Gabor spatial feature space of images by generalizing the inverse edge indicator function $E$, which attracts in turn the evolving curve towards the boundary in the classical and geodesic snakes schemes. A special feature of our approach is the metric introduced in the Gabor space, and used as the building block for the stopping function $E$ in the geodesic active contours scheme.

Sochen et al [22] proposed to view images and image feature space as Riemannian manifolds embedded in a higher dimensional space. For example, a gray scale image is a 2-dimensional Riemannian surface (manifold), with $(x, y)$ as local coordinates, embedded in $\mathbb{R}^3$ with $(X, Y, Z)$ as local coordinates. The embedding map is $(X = x, Y = y, Z = I(x, y))$, and we write it, by abuse of notations, as $(x, y, I)$. When we consider feature spaces of images, e.g. color space, statistical moments space, and the Gaborian space, we may view the image-feature information as a $N$-dimensional manifold embedded in a $N + M$ dimensional space, where $N$ stands for the number of local parameters needed to index the space of interest and $M$ is the number of feature coordinates. For example, we may view the Gabor transformed image as a 2D manifold with local coordinates (x,y) embedded in a 6D feature space. The embedding map is $(x, y, \theta(x, y), \sigma(x, y), R(x, y), J(x, y))$, where R and J are the real and imaginary parts of the Gabor transform value, and $\theta$ and $\sigma$ as the direction and scale for which a maximal response has been achieved. Alternatively, we can

represent the transform space as a 4D manifold with coordinates $(x, y, \theta, \sigma)$ embedded in the same 6D feature space. The embedding map, in this case, is $(x, y, \theta, \sigma, R(x, y, \theta, \sigma), J(x, y, \theta, \sigma))$. The main difference between the two approaches is whether $\theta$ and $\sigma$ are considered to be local coordinates or feature coordinates. In any case, these manifolds can evolve in their embedding spaces via some geometric flow.

A basic concept in the context of Riemannian manifolds is distance. For example, we take a two-dimensional manifold $\Sigma$ with local coordinates $(\sigma_1, \sigma_2)$. Since the local coordinates are curvilinear, the distance is calculated using a positive definite symmetric bilinear form called the metric whose components are denoted by $g_{\mu\nu}(\sigma_1, \sigma_2)$:

$$ds^2 = g_{\mu\nu} d\sigma^\mu d\sigma^\nu, \tag{9}$$

where we used the Einstein summation convention : elements with identical superscripts and subscripts are summed over.

The metric on the image manifold is derived using a procedure known as pullback. The manifold's metric is then used for various geometrical flows. We shortly review the pullback mechanism. More detailed information can be found in [22].

Let $X : \Sigma \to M$ be an embedding of $\Sigma$ in $M$, where $M$ is a Riemannian manifold with a metric $h_{ij}$ and $\Sigma$ is another Riemannian manifold. We can use the knowledge of the metric on $M$ and the map $X$ to construct the metric on $\Sigma$. This pullback procedure is as follows:

$$(g_{\mu\nu})_\Sigma(\sigma^1, \sigma^2) = h_{ij}(X(\sigma^1, \sigma^2)) \frac{\partial X^i}{\partial \sigma^\mu} \frac{\partial X^j}{\partial \sigma^\nu}, \tag{10}$$

where we used the Einstein summation convention, $i, j = 1, \ldots, dim(M)$, and $\sigma^1, \sigma^2$ are the local coordinates on the manifold $\Sigma$.

If we pull back the metric of a 2D image manifold from the Euclidean embedding space (x,y,I) we get:

$$(g_{\mu\nu}(x, y)) = \begin{pmatrix} 1 + I_x^2 & I_x I_y \\ I_x I_y & 1 + I_y^2 \end{pmatrix}. \tag{11}$$

The determinant of $g_{\mu\nu}$ yields the expression : $1 + {I_x}^2 + {I_y}^2$. Thus, we can rewrite the expression for the stopping term $E$ in the geodesic snakes mechanism as follows:

$$E(|\nabla I|) = \frac{1}{1 + |\nabla I|^2} = \frac{1}{\det(g_{\mu\nu})}.$$

We may interpret the Gabor transform of an image as a function assigning for each pixel's coordinates, scale and orientation, a value (W). Thus, we may view the Gabor transform of an image as a 4D manifold with local coordinates $(x, y, \theta, \sigma)$ embedded in $\mathbb{R}^6$ of coordinates $(x, y, \theta, \sigma, R, J)$. We may pull back the metric for the 4D manifold from the 6D space, and use it to generate the stopping function $E$ for the geodesic snakes mechanism. The metric derived for the 4D manifold is:

$$(g_{\mu\nu}) = \begin{pmatrix} 1+R_x^2+J_x^2 & R_xR_y+J_xJ_y & R_xR_\theta+J_xJ_\theta & R_xR_\sigma+J_xJ_\sigma \\ R_xR_y+J_xJ_y & 1+R_y^2+J_y^2 & R_yR_\theta+J_yJ_\theta & R_yR_\sigma+J_yJ_\sigma \\ R_xR_\theta+J_xJ_\theta & R_yR_\theta+J_yJ_\theta & 1+R_\theta^2+J_\theta^2 & R_\theta R_\sigma+J_\theta J_\sigma \\ R_xR_\sigma+J_xJ_\sigma & R_yR_\sigma+J_yJ_\sigma & R_\theta R_\sigma+J_\theta J_\sigma & 1+R_\sigma^2+J_\sigma^2 \end{pmatrix} \tag{12}$$

The resulting stopping function $E$ is the inverse of the determinant of $g_{\mu\nu}$. Here $g_{\mu\nu}$ is a function of four variables ($x, y, \theta$ and $\sigma$), therefore, we obtain an evolution of a 4D manifold in a 6D embedding space.

Alternative approach is to derive a stopping term $E$ which is a function of $x$ and $y$ only. One way to achieve this is to get the scale and orientation for which we have received the maximum amplitude of the transform for each pixel. Thus, for each pixel, we obtain: $W_{max}$, the maximum value of the transform, $\theta_{max}$ and $\sigma_{max}$ – the orientation and scale that yielded this maximum value. This approach results in a 2D manifold (with local coordinates $(x, y)$) embedded in a 6D space (with local coordinates $(x, y, R(x, y), J(x, y), \theta(x, y), \sigma(x, y))$. If we use the pullback mechanism described above we get the following metric:

$$(g_{\mu\nu}) = \begin{pmatrix} 1+R_x^2+J_x^2+\sigma_x^2+\theta_x^2 & R_xR_y+J_xJ_y+\sigma_x\sigma_y+\theta_x\theta_y \\ R_xR_y+J_xJ_y+\sigma_x\sigma_y+\theta_x\theta_y & 1+R_y^2+J_y^2\sigma_x^2+\theta_x^2 \end{pmatrix} \tag{13}$$

Again, we use the fact that the determinant of the metric is a positive definite edge indicator to determine $E$ as the inverse of the determinant of $g_{\mu\nu}$. Here $g_{\mu\nu}$ is a function of the two spatial variables only $x$ and $y$, therefore, we obtain an evolution of a 2D manifold in a 6D embedding space.

## 5 Results and Discussion

Geodesic snakes provide an efficient geometric flow scheme for boundary detection, where the initial conditions include an arbitrary function $U$ which implicitly represents the curve, and a stopping term $E$ which contains the information regarding the boundaries in the image. Gabor filters are optimally tuned to localized scale and orientation, and can therefore represent textural information. We actually generalize the definition of gradients which usually refers to intensity gradients over $(x, y)$ to other possible gradients in scale and orientation. This gradient information is the input function $E$ to the newly generalized geodesic snakes flow.

In our application of geodesic snakes to textural images, we have used the mechanism offered by [15] to generate the Gabor wavelets for five scales and four orientations in a frequency range of $0.1 - 0.4$ cycles per pixel. We note that this choice is different from the usual scheme in vision, where there are four scales and at least six orientations in use. In the geodesic snakes mechanism $U$ was initiated to be a signed distance function [2].

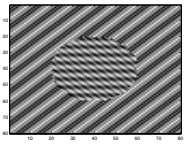

**Fig. 1.** A synthetic image made up of 2D sinewave gratings of different frequencies and orientations

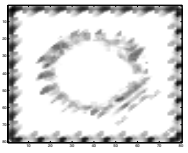

**Fig. 2.** The stopping function $E$ calculated by means of the 2D manifold metric

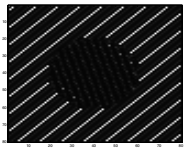

**Fig. 3.** The stopping function $E$ of the first image calculated by using the intensity based definition $E(I) = \frac{1}{1+|\nabla I|^2}$

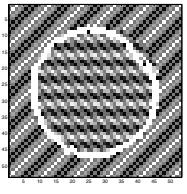

**Fig. 4.** The resultant boundary

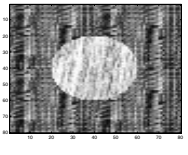

**Fig. 5.** An image comprised of two textures are taken from Brodatz album of textures [1]

We present the results of the 2D manifold approach for a synthetic image: the original image, the resulting stopping term $E$ and the final boundary detected. We present some preliminary results for the 4D manifold approach with a Brodatz image: the resultant $E$ is projected on the X-Y plane for each scale and orientation.

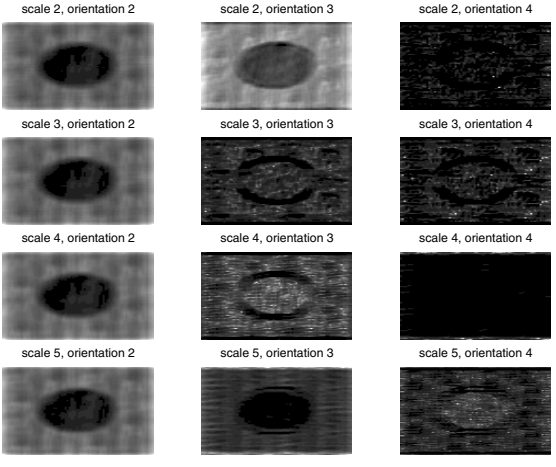


**Fig. 6.** The stopping function $E$ for the Brodatz texture image, calculated by using the 4D manifold metric. For full size images see the web-page: **http://www-visl.technion.ac.il/gaborsnakes**

The first image (Fig. 1) is a synthesized texture composed of linear combination of spatial sinewave gratings of different frequencies and orientations. When the stopping term $E$ is calculated using the $2D$ manifold metric, we obtain a clear picture of the texture gradients (i.e. where significant changes in texture occur) in the image (Fig. 2). So, our initial contour is drawn to the wanted boundary. As can be seen in figure (3), when $E$ is calculated using intensity values only, $E(I) = \frac{1}{1+|\nabla I|^2}$, the texture gradients are not visible, and the resultant $E$ will probably not attract the initial contour towards the boundary. Application of the geodesic snakes algorithm using the 2D manifold approach results in an accurate boundary, as can be seen in figure (4).

When we consider the entire Gabor spatial feature space, the stopping term $E$ is a function of four variables $x, y, \theta$, and $\sigma$. In more complex (texture-wise) images such as the Brodatz textures (Fig. 5), taken from [1], we may see the additional information that can be obtained. In figure (6) we present $E$ as calculated for five scales and four orientations; however, only the components containing significant information is presented in the figure. We can see that information is preserved through scales. The $E$ function contains more information when it is calculated by using the 4D manifold approach than the $E$ function obtained by

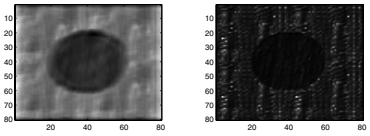


**Fig. 7.** The stopping function $E$ used in the application of the proposed scheme to the Brodatz image using: (left) the 4D manifold approach incorporating specific scale and orientation (right) the intensity based definition $E(I) = \frac{1}{1+|\nabla I|^2}$

using the intensity based approach (Fig.7). In other words, we obtain a clear division of the image into two segments, which differ in their texture, and thereby get information about the relevant edges. As our main goal is to determine the boundaries in the image, we may deconvolve $E$ for each scale and orientation with an appropriate gaussian function in order to obtain better spatial resolution.

The proposed texture segmentation scheme applies the geodesic active contours algorithm to the Gabor space of images, while the original geodesic snakes implements intensity gradients. The implementation of the feature space of images results in detection of texture gradients. We treat the Gabor transformed image as a 2D manifold embedded in a 6D space, or a 4D manifold embedded in a 6D space, and calculate the local metric on the manifold using the pullback method. We then integrate the metric information to the geodesic snakes scheme. We have shown the feasibility of the proposed approach, and its advantages over the intensity geodesic snakes applied to multi-textured images. This is currently further extended by completing the application of geodesic snakes to a 4D manifold (x,y,$\theta$,$\sigma$) embedded in a 6D space (R,J,x,y,$\theta$,$\sigma$), and by the application of both schemes to medical images.

## Acknowledgements

This research has been supported in part by the Ollendorff Minerva Center of the Technion, by the Fund for Promotion of Research at the Technion, and by the Consortium for Broadband Communication, administrated by the Chief Scientist of the Israeli Ministry of Industry and Commerce.

## References

1. P. Brodatz, Textures: A photographic album for Artists and Designers, New York, NY, Dover, 1996.
2. V. Caselles and R. Kimmel and G. Sapiro, "Geodesic Active Contours", *International Journal of Conputer Vision*, 22(1), 1997, 61-97.
3. R. Conners and C. Harlow "A Theoretical Comparison of Texture Algorithms"*IEEE Transactions on PAMI*, 2, 1980, 204-222.

4. G. R. Cross and A. K. Jain, "Markov Random Field Texture Models" *IEEE Transactions on PAMI*, 5, 1983, 25-39.
5. J. G. Daugman, "Uncertainty relation for resolution in space, spatial frequency, and orientation optimized by two-dimensinal visual cortical filters", *J. Opt. Soc. Amer.* 2(7), 1985, 1160-1169.
6. D. Gabor "Theory of communication"*J. IEEE* , 93, 1946, 429-459.
7. S. Geman and D. Geman "Stochastic relaxation, Gibbs distribution and the Bayesian restoration of images", *IEEE Transactions on PAMI*, 6, 1984, 721-741.
8. B. Julesz "Texton Gradients: The Texton Theory Revisited", *Biol Cybern*, 54, (1986) 245-251.
9. M. Kaas, A. Witkin and D. Terzopoulos, "Snakes : Active Contour Models", *International Journal of Computer Vision*, 1, 1988, 321-331.
10. R. Kimmel, R. Malladi and N. Sochen, "Images as Embedding Maps and Minimal Surfaces: Movies, Color, Texture, and Volumetric Medical Images",*Proc. of IEEE CVPR'97*, (1997) 350-355.
11. R. Kimmel, N. Sochen and R. Malladi, "On the geometry of texture", Proceedings of the 4th International conference on Mathematical Methods for Curves and Surfaces, St. Malo, 1999.
12. T. S. Lee, "Image Representation using 2D Gabor-Wavelets", *IEEE Transactions on PAMI*, 18(10), 1996, 959-971.
13. T. S. Lee, D. Mumford and A. Yuille, "Texture segmentation by minimizing vector-valued energy functionals: the coupled-membrane model", *Lecture Notes in Computer Science, Computer Vision ECCV 92*, 588, Ed. G. Sandini, Springer-Verlag, 165-173.
14. L. M. Lorigo, O. Faugeras, W. E. L. Grimson, R. Keriven, R. Kikinis, "Segmentation of Bone in Clinical Knee MRI Using Texture-Based Geodesic Active Contours", *Medical Image Computing and Computer-Assisted Intervention*, 1998, Cambridge, MA, USA.
15. B. S. Manjunath and W. Y. Ma, "Texture features browsing and retrieval of image data", *IEEE Transactions on PAMI*, 18(8), 1996, 837-842.
16. S. Marcelja, "Mathematical description of the response of simple cortical cells", *J. Opt. Soc. Amer.*, 70, 1980, 1297-1300.
17. J. Morlet, G. Arens, E. Fourgeau and D. Giard, "Wave propagation and sampling theory - part 2: sampling theory and complex waves", *Geophysics*, 47(2), 1982, 222 - 236.
18. N. Paragios and R. Deriche, "Geodesic Active Regions for Supervised Texture Segmentation", *Proceedings of International Conference on Computer Vision*, 1999, 22-25.
19. M. Porat and Y. Y. Zeevi, "The generalized Gabor scheme of image representation in biological and machine vision", *IEEE Transactions on PAMI*, 10(4), 1988, 452-468.
20. M. Porat and Y. Y. Zeevi, "Localized texture processing in vision: Analysis and synthesis in the gaborian space", *IEEE Transactions on Biomedical Engineering*, 36(1), 1989, 115-129.
21. S. J. Osher and J. A. Sethian, "Fronts propagating with curvature dependent speed: Algorithms based on Hamilton-Jacobi formulations", *J of Computational Physics*, 79, 1988, 12-49.
22. N. Sochen, R. Kimmel and R. Malladi , "A general framework for low level vision", *IEEE Trans. on Image Processing*, 7, (1998) 310-318.
23. M. Zibulski and Y. Y. Zeevi, "Analysis of multiwindow Gabor-type schemes by frame methods", *Applied and Computational Harmonic Analysis*, 4, 1997, 188-221.